

Dispersion of dust sizes in the plasma of aluminum dust flame

J. A. Doroshenko, N. I. Poletaev, and V. I. Vishnyakov
Mechanik Odessa National University, Odessa 65026, Ukraine

(Received 9 April 2009; accepted 25 August 2009; published online 8 September 2009)

The result of an experimental study of the dispersion of sizes of alumina particles, obtained as a result of condensation in the thermal plasma formed in the two-phase diffusion flame of a burning aluminum dust cloud, is presented. The decrease in the average size of condensed particles and the size dispersion when the temperature of the flame increases is demonstrated. © 2009 American Institute of Physics. [doi:10.1063/1.3227801]

The development of modern technologies demands the new materials, such as the ultradisperse particles of metal oxides. Such particles, with the size about 10 nm, are necessary for making flexible ceramics, which will possess sufficient malleability for replacement of metal components in the various devices operating at high temperatures, for example, core engine, gas turbines, and rocket engines.^{1,2} Another important direction of application of the ultradisperse oxide particles is the manufacturing of fuel cells.³ The nanosize particles of alumina are used for manufacturing abrasives; the nanosize particles of iron oxide are used for manufacturing thin magnetic fluids.⁴ Additionally, particles with sizes under 10 nm have unique properties that are not studied enough.

However there are technological difficulties in obtaining nanosize powders. For this purpose expensive chemical methods are mostly used. Recently the attention of technologists was attracted to the opportunity of obtaining nanosize particles of metal oxides as a result of condensation of combustion products in the dust flame—the so-called gas-dispersion synthesis.⁵

The main idea of the gas-dispersion synthesis method is that the gas mixture of the metal powder (or mechanical intermixture of metals) is burnt in the oxidizing environment for which a self-supporting laminar two-phase flame can be formed. The combustion products (oxide particles) condensing outside the zone of burning have preferentially bimodal distribution of particles by sizes, i.e., consist of two fractions; one of which has a maximum of distribution in the range of the sizes much exceeding 1 μm , another in the range of 1–50 nm. Therefore the gas mixture of combustion products is forced through the double filter. The first section of this filter hits back a large dispersion fraction while a small dispersion fraction settles down on the second section.

There are the following advantages of the gas-dispersion synthesis technology: (i) the possibility to obtain metal oxides of high chemical purity as a result of the self-cleaning of the product in the zone of burning; (ii) exceptionally low energy capacity due to the self-supporting mode of burning requiring no external source of energy; (iii) high ecological cleanliness due to the absence of by-products that require utilization.

It should be noted that nucleation occurs in the thermal dust-electron plasma which was formed in the zone of com-

bustion products. This plasma consists of a gas at atmospheric pressure and solid or liquid particles of metal oxide which emits electrons. It is clear that the presence of free electrons influences the process of nucleation.

In Ref. 6 the theoretical model of formation of the dust grain nucleation centers in dust-electron plasmas within the limits of the classical theory of homogeneous nucleation has been presented. In this theory it is considered that the dust grain nucleation centers in the plasma get a charge via the thermionic emission and via the interaction with the plasma electrons. The interior free energy of the dust grain nucleation centers and the superficial tension are dependent on their charges. The ratio of critical radius of the charged nucleation center to the neutral nucleation center is described by the following expression:

$$\frac{r_{\text{cr}}}{r_0} = \frac{1}{2} + \frac{1}{2} \left\{ 1 - \frac{\sqrt{2}k_B T}{2\pi\gamma_0 r_0 e^2} \times \left[k_B T \int_0^{V_{bn}/k_B T} \sqrt{\exp(x) - x - 1} dx + \text{sgn}(V_{bn}) \times \left(W_n + \frac{3}{2}k_B T \right) \sqrt{\exp\left(\frac{V_{bn}}{k_B T} - \frac{V_{bn}}{k_B T} - 1\right)} \right] \right\}^{1/2},$$

where T is the Kelvin temperature, k_B is the Boltzmann constant, γ_0 is the superficial tension of neutral nucleation center, W_n is the electronic work function from nucleation center, and V_{bn} is the potential barrier on the nucleation center-plasma boundary.

It has been demonstrated that the interaction of the dust nucleation centers with the plasma electrons leads to the formation of a self-consistent system, which stabilizes the size of nucleation centers. This theory predicts that the increasing of the temperature of plasma leads to the decrease in the size of nucleation centers and which is remarkable to the decrease in the dispersion of the sizes of nucleation centers.

To check these theoretical predictions, the experiments, which results are presented in this paper, have been made. We should note that in Ref. 6 only nucleation was considered, but not a growth of dust, therefore only comparison of the tendencies in theory and experiment is possible.

The object of research was the disperse structure of the combustion products of aluminum dust cloud in the laminar two-phase flame. The influence of the concentration of the

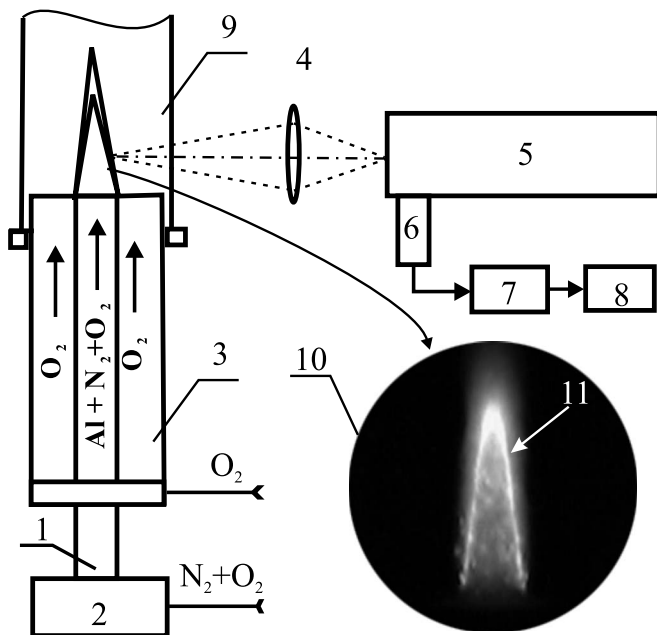


FIG. 1. Diagram of experimental device: (1) inner burner tube, (2) dispersion unit, (3) outer burner tube, (4) lens, (5) spectral device, (6) photodetector (FEM-106), (7) oscilloscope, (8) video camera, (9) protective quartz pipe, (10) photograph of the two-phase aluminum flame, and (11) condensation zone.

oxidizing agent in carrier gas, which defines the temperature of the flame, on the disperse structure of ultradisperse fractions of aluminum combustion products was explored. The schematic of the experimental device is present in Fig. 1.⁷ The laminar two-phase flame of an aluminum dust cloud has been obtained using a “dusty torch”,^{8,9} consisting of two vertical coaxial cylinders. The aluminum dust cloud was introduced into the interior pipe by the carrier gas (a mix of nitrogen with variable impurity of oxygen). The oxidizing gas (pure oxygen) was supplied into the ring backlash between the exterior and interior pipes. The oxygen blow is necessary to ensure complete combustion of the aluminum particles at low concentration of oxygen in the carrier gas. With such an arrangement of the dust cloud burning the double flame is formed: The interior is the premixed flame,^{10,11} the exterior is the diffusion flame¹² in which the afterburning occurs.

The condensed-phase temperature at the flame front was determined by a multiwave method.¹³ The device (5) on the basis of interference wedges was used for the flame diagnostics on the continuous spectrum in the range $\lambda = (0.45-1.1)\mu$. The rotating interference wedges gave the possibility to detect up to 100 spectra/s with the spectral resolution $\Lambda=20-60$. The spectral device was calibrated in terms of wavelength by a mercury lamp and in terms of intensity by a SI10-300 tungsten band lamp. The spectral luminosity (r_λ) of the aluminum dust flame is shown in Fig. 2.

Using the Wein equation for the spectral intensity, measurement data on the spectral luminosity of the flame over a wide spectral interval were used to plot the dependence of $\ln(r_\lambda \lambda^5)$ on $1/\lambda$. In the wavelength interval in which the plot

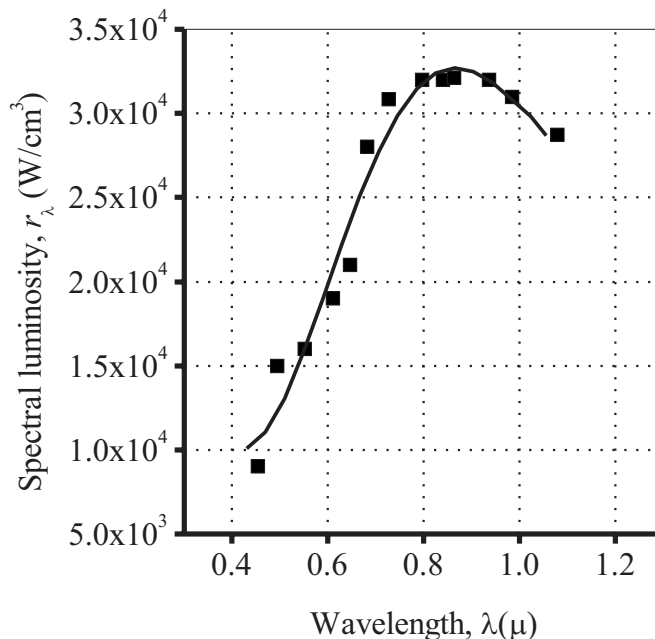


FIG. 2. The spectral luminosity of the aluminum dust flame: dots are the experiment data and solid line is the polynomial curve fit.

is a straight line (see Fig. 3), the radiation can be considered gray, which allowed the true temperature to be determined from the slope of this straight line to the abscissa. The average condensed-phase temperature was determined by processing of 15–20 spectra.

The mass density of the aluminum particles in the cloud was $4 \times 10^{-4} \text{ g/cm}^3$ in all cases; the median diameter of particles was 4.8μ . The volumetric flow rates were $800 \text{ cm}^3/\text{s}$ for the oxidizing gas and $300 \text{ cm}^3/\text{s}$ for the carrier gas. The measurements were carried out at three values of the content of oxygen in the carrier gas: $C_1=6.4\%$, C_2

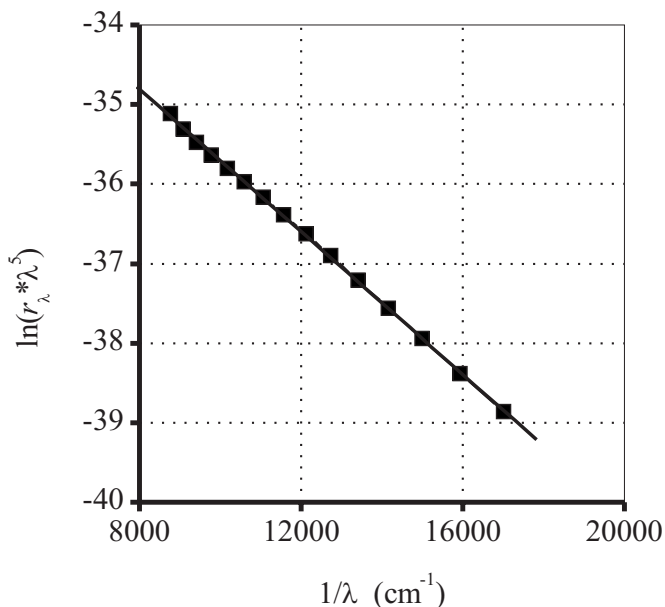


FIG. 3. The dependence of $\ln(r_\lambda \lambda^5)$ on $1/\lambda$ for the aluminum dust flame: dots are the experiment data and solid line is the polynomial curve fit.

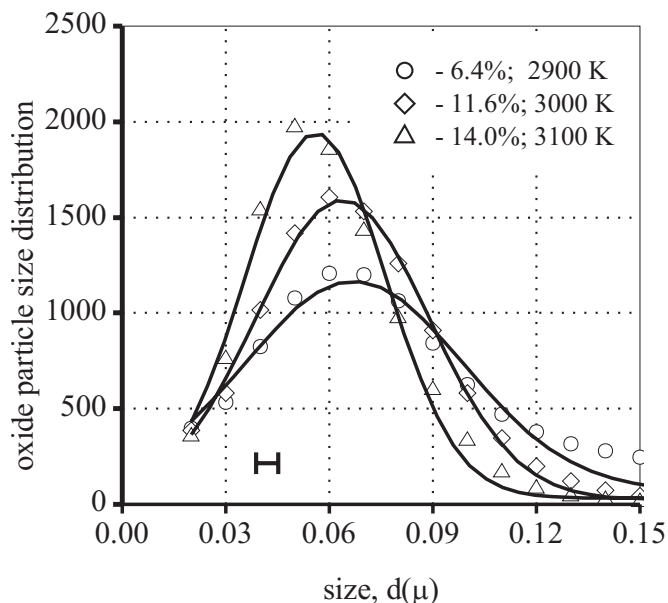


FIG. 4. Size distribution of the alumina dust: dots are the experiment data and solid line is the Gaussian curve fit.

=11.6%, and $C_3=14.0\%$ that correspond to the temperature of flame $T_1 \sim 2900$ K, $T_2 \sim 3000$ K, and $T_3 \sim 3100$ K accordingly.

The x-ray analysis of the combustion products has shown that the particles have crystalline structure of γ - Al_2O_3 . The chemical analysis has shown 99.95% content of alumina in the condensed dust particles. The fine fraction of alumina dust (settled on the filters) was studied using the electronic microscope, which allowed to conduct the disperse analysis of the condensed particles and to plot the size distribution of dust particles¹⁴ presented in Fig. 4.

The increase in the oxygen content in the carrier gas and, accordingly, the increase in the temperature of the plasma lead to the decrease in the size of alumina condensed particles, which is well visible in Fig. 4—the maximum of the size distribution shifts to the range of smaller sizes. At the same time, there is a decrease in the dispersion of distribution that is well visible in Table I.

Thus, the increase in the temperature of plasma leads to

TABLE I. The average diameter d and the width of distribution σ .

O_2 (%)	$T(K)$	$d(\mu)$	$\sigma(\mu)$
6.4	2900	0.067	0.064
11.6	3000	0.064	0.050
14.0	3100	0.056	0.041

the decrease in the average size of the condensed alumina particles and to the decrease in the dispersion of the sizes as well. These effects completely correspond to the tendency of theoretical model Ref. 6 and allow to conclude that in the premixed aluminum dust flame, there is a homogeneous condensation of aluminum oxide particles from the vapor phase which can be described within the limits of the theory of homogeneous condensation.

¹C. A. Laurvick and B. Singaraju, *Proceedings of the 21st Digital Avionics Systems Conference*, Irvine, CA, October 2002 (IEEE, Piscataway, 2002), Vol. 2, p. 9A3-1.

²J.-P. Borra, *J. Phys. D* **39**, R19 (2006).

³*Handbook of Fuel Cell Technology*, edited by W. Vielstich, A. Lamm, and H. Gasteiger (Wiley, New York, 2002).

⁴Z. Z. Xu, C. C. Wang, W. L. Yang, Y. H. Deng, and S. K. Fu, *J. Magn. Magn. Mater.* **277**, 136 (2004).

⁵A. N. Zolotko, Ya. I. Vovchuk, N. D. Ageev, and S. V. Goroshin, USSR Patent No. 1832397, 1993.

⁶V. I. Vishnyakov, *Phys. Rev. E* **78**, 056406 (2008).

⁷N. I. Poletaev and A. V. Florcko, *Combust., Explos. Shock Waves* **44**, 437 (2008).

⁸A. N. Zolotko, Ya. I. Vovchuk, N. I. Poletaev, A. V. Florcko, and I. S. Altman, *Combust., Explos. Shock Waves* **32**, 262 (1996).

⁹N. I. Poletaev, A. N. Zolotko, A. V. Florcko, Ya. I. Vovchuk, and A. A. Nazarenko, in *Proceeding of the Third European Congress of Chemical Engineering*, Nuremberg, 26–28 June 2001, CD-ROM, available from VDI-DECHEMA, Dusseldorf.

¹⁰A. Lemaire, T. Meyer, K. Zähringer, J. Gord, and J. Rolon, *Exp. Fluids* **36**, 36 (2004).

¹¹Yu. S. Naiborodenko and V. I. Itin, *Fiz. Gorenia i Vzryva (USSR)* **11**, 293 (1975).

¹²N. D. Ageev, Ya. I. Vovchuk, S. V. Goroshin, A. N. Zolotko, and N. I. Poletaev, *Combust., Explos. Shock Waves* **26**, 669 (1990).

¹³B. Block, W. Hentschel, and W. Ertmer, *Combust. Flame* **114**, 359 (1998).

¹⁴A. N. Zolotko, N. I. Poletaev, J. I. Vovchuk, and A. V. Florcko, in *Gas Phase Nanoparticle Synthesis*, edited by C. G. Granqvist, L. B. Kish, and W. H. Marlow (Kluwer Academic, Dordrecht, 2004), Chap. 5, pp. 123–156.